Electronic supplementary information

Conversion of Inert Cryptomelane-type Manganese Oxide into A Highly Efficient Oxygen Evolution Catalyst via Limited Ir Doping

Wei Sun[1], Li-mei Cao[1], Ji Yang[1],*

[1]State Environmental Protection Key Laboratory of Environmental Risk Assessment and Control on Chemical Processes, School of Resources and Environmental Engineering, East China University of Science and Technology, 130 Meilong Road Shanghai 200237, P.R. China,

*Corresponding authors' E-mail: yangji@ecust.edu.cn

Experimental Section

Materials synthesis: The materials of IrO_2, cryptomelane(Ir) (named as cry-Ir), cryptomelane (named as cry-Mn), Mn_2O_3 and $Ir_xMn_{1-x}O_2$ are synthesized via hydrothermal method which modified from our previous work[1]. The prepared materials are annealed at 450-600°C with a dwell time of 6-h to produce good crystallinity. For preparing cry-Mn, 0.1 M of 6 mL aqueous potassium permanganate ($KMnO_4$; analytically pure, Shanghai Ling Feng Chemical Reagent Co.,Ltd) is mixed with 0.5 mL 0.5 M HCl (analytically pure，Shanghai Ling Feng Chemical Reagent Co.,Ltd) and later 10 mL deionized water is added. The purpose of HCl addition is to retain certain acidity, as it will react with the produced KOH from reaction to accelerate the hydrothermal reaction of $KMnO_4$. The hydrothermal temperature is maintained at 200°C for 480 min. The product yield in mass of cry-Mn is about 80 mg. To prepare cry-Ir, 8 mL of 0.1 M $KMnO_4$ as an oxidant is mixed with 2 mL 56.7 mmol/L iridium trichloride ($IrCl_3·3H_2O$; analytically pure, TCI (shanghai) Development Co.,Ltd) as reductant with subsequent addition of 10 mL deionized water. In order to figure out the optimal synthesis condition, cry-Ir is respectively prepared at two different temperatures of 150°C and 200°C for 480 min, and it appeared that 200°C is the optimum hydrothermal temperature for cry-Ir synthesis. After hydrothermal reaction, the solution pH falls into the range of 8.14-8.78. The yield for cry-Ir is ~160 mg. Mn_2O_3 is prepared by mixing $KMnO_4$ (4 mL 0.1 M) and $MnCl_2$ (6 mL 0.1 M, analytically pure, Shanghai Ling Feng Chemical Reagent Co.,Ltd) with 10 mL deionized water, and further adding 0.5 mL of 0.5 M HCl to adjust its acidity. The hydrothermal temperature is set at 200°C for a dwell time of 480 min. We obtain ~80 mg mass of Mn_2O_3. The $Ir_xMn_{1-x}O_2$ materials are prepared by variable stoichiometric Ir/Mn mole ratios (the concentration of $IrCl_3·3H_2O$ is 56.7 mM and the used $Mn(NO_3)_2$ (analytically pure, Shanghai Ling Feng Chemical Reagent Co.,Ltd) is 113.4 mM aqueous) mixed with 10 mL deionized water and further adding 5 mL of 0.5 M aqueous NaOH (analytically pure, Shanghai Ling Feng Chemical Reagent Co.,Ltd). The product mass of $Ir_xMn_{1-x}O_2$ materials lies in the range of 40 mg to 60 mg, depending upon the volume of precursors. All materials are added into a 40-mL Teflon-lined pressure vessel, later was loaded into an oven to heat the solution to different set conditions of temperature and time; then, the vessels were cooled naturally at room temperature. The precipitates were suction filtered and washed with deionized water at least twice to remove other ions. The remaining solid on the filter was dried to dehydration in an oven at 80 °C for 1 h. The dried solid was transferred to a crucible and annealed at 450 °C for Mn_2O_3 and 600 °C for other materials with 6 h to produce excellent crystallinity.

Electrode Preparation and Electrochemical Measurements. In this study, the electrodes used for the electrochemical measurements were of the so-called dimensionally stable anode (DSA) type, which were prepared as follows. 6 mg of fresh catalyst powders were dispersed in 1.5 mL of 2:1 v/v isopropanol / water and then ultrasonicated for approximately 1 h to form a homogeneous ink. Next, 7.5 µL of ink deposited on 0.5 cm × 1.5 cm Ti plate, which was etched for 2 h by 10% (wt %) oxalic acid under near boiling conditions and then washed with deionized water. The

process was repeated 5 times to obtain a loading weight of approximately 0.2 mg/cm^2 and was then stabilized by annealing for 20 minutes at 400 °C on each cycle. All electrochemical measurements were conducted using a three–electrode cell. The working electrode used was 0.5 cm × 0.5 cm (electrode reactive area = 0.25 cm^2) of the prepared DSA, and the remaining was insulated, except for a small part for connecting the wire. Here, a saturated calomel reference electrode (SCE) and a polished and cleaned Pt foil with a 1 cm × 1 cm reaction area were used for the counter electrode. The electrode potential from the SCE scale was converted to the reversible hydrogen electrode (RHE) scale by calibrating with: E (NHE) = E (SCE) + E$_{j=0}$. The over-potential values (η) corrected with the iR were obtained using the following equation: η = E$_{Applied}$ (RHE) – iR-1.229, where i is the current, and R is the uncompensated Ohmic electrolyte resistance and was measured via electrochemical workstation (CH Instruments Ins., CHI660E) at the open circuit 10 mV potential in 0.1M HClO$_4$ solutions. The working electrodes were cycled a least 5 times until the curves were observed to overlap; then, the data of the CV's and polarization curves were recorded at the specified scan rate. The Tafel plots were conducted by the stair-case voltammetry method at the different potential range (vs. RHE), with 10 mV steps every 100 s (scan rate 0.1 mV/s) and current values were read at the end of each step. The electrolytes used were 0.1 M HClO$_4$ (pH~1), and all chemicals used were of analytical grade, and the solvent used was deionized water.

Characterization. The materials surface area are evaluated by BET method on a Micromeritics Tristar 3020. The crystal structure of the catalysts were investigated using powder X-Ray diffraction (XRD) using a D/max2550 V apparatus with a Cu-Kα radiation source (λ=1.5406 Å), and the data were recorded over a range of 10 to 80° at a step size of 0.02°. The morphologies of the catalysts were observed using a field-emission scanning electron microscope (FESEM) equipped with a Nova NanoS and the Energy dispersive X-ray (EDX) spectrometer to confirm the composition using a TEAMApollo system. A JEM-2100 transmission electron microscope was used to obtain the TEM and HRTEM images. The surface properties of the catalysts were determined via X-ray photoelectron spectroscopy (XPS) and valence band spectra (VBS) using an ESCALAB 250Xi instrument with an Al-Kα radiation source at an energy step size of 0.05 eV for high resolution XPS spectrum. The samples were sputter coated with carbon, and the spectra were calibrated with respect to C-*1s* at a binding energy of 284.6 eV. The X-ray absorption data (XAS) at the Ir L_{III} edge and the Cu *K* edge of the samples, which were mixed with LiF to reach 50 mg, were recorded at room temperature in transmission mode using ion chambers using the BL14W1 beam line of the Shanghai Synchrotron Radiation Facility (SSRF), China. The station was operated with a Si (111) double crystal monochromator. During measurements, the synchrotron was operated at an energy of 3.5 GeV and a current between 150-210 mA.

ICP experiments: The samples of cryptomelane(Ir) are by microwave digestion treatment. First, the samples are mixed within 4 mL concentrated HNO$_3$ and 1 mL concentrated HCl in digestion tanks. Then, we perform two step digestion process, the tanks are heating to 150°C by a half hour and dwell 60 min, and next heating to

170°C in 20 min and dwell 60 min. The all samples are constant volume to 50 mL and the color is light brown.

RHE calibration: The SCE was calibrated with respect to the RHE in all three types of pH solution using a high purity hydrogen saturated electrolyte with a Pt foil as the working electrode. CVs were run at a scan rate of 5 mV/s, and the average of the two potentials at which the current crossed zero was recorded to as the thermodynamic potential for the hydrogen electrode reaction.

TOF calculation:

The values of TOF at $\eta=0.340$ V were calculated by assuming that every Ir atom is the active site in catalysts rather than Mn site and this be discussed in main text.

$$TOF = \frac{j\,A_{geo}}{4\,F\,n}$$

In here, the j is the current density (mA cm^{-2}) at the $\eta=0.340$ V; A_{geo} is geometric area of electrode is 0.25 cm^2; the number 4 means the 4 electrons transfer process of OER; the F is Faraday's constant and the value is 96485.3 C mol^{-1}; the number n is moles of Ir atom in loading catalysts on electrodes, for cry-Ir, the chemical formula is given by $K_{1.65}(Mn_{0.78}Ir_{0.22})_8O_{16}$.
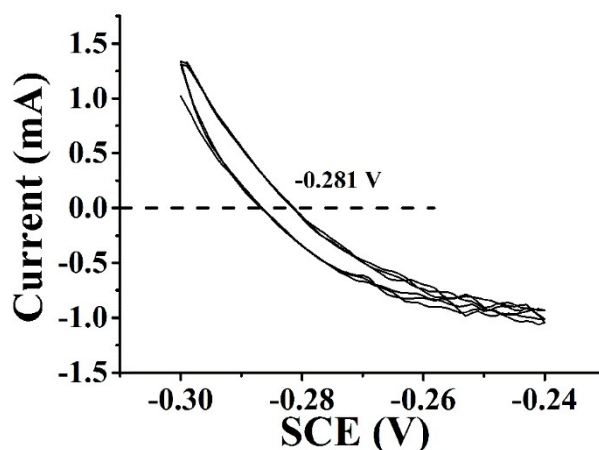
CVs for RHE Calibration in acid solution 0.1M HClO$_4$ pH ~ 1. So, the

RHE=SCE+0.281 V for acid solution.

Table S1. The EDS and ICP data of cryptomelane(Ir).

Samples	EDS (wt%)			ICP (mg/L)			Ir/Mn (ICP)
	K	Ir	Mn	K	Ir	Mn	
1	8.00	29.55	41.95	2.2	12	11.9	0.288

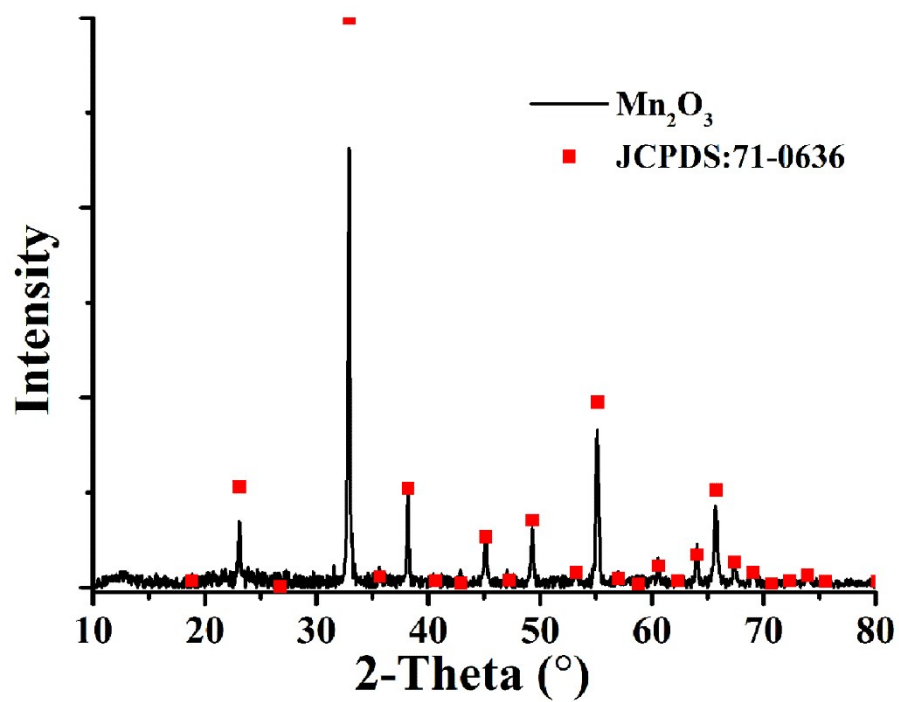|							
2	7.72	29.22	43.05	2.3	11.8	11.9	0.284
3	7.64	27.9	45.07	2.6	13	13	0.286
4	7.57	29.03	38.78	2.5	12.5	12.7	0.282

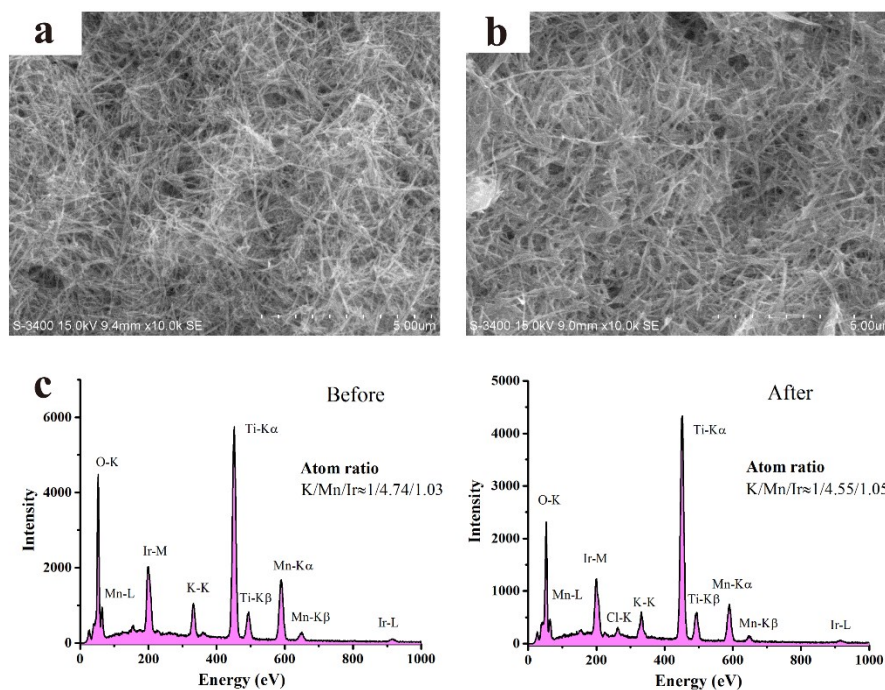**Fig. S1.** XRD pattern for Mn_2O_3. We can find that it totally agree with ICPDS:71-0603.

Fig. S2. (a) and (b) are the SEM images of fresh catalyst anchored on Ti before OER activity test and after. (c) Elements EDS spectra corresponding to the fresh one and after test. From the spectra, we can find that the K/Mn/Ir atomic ratio has a litter change, and the Cl has been determined mainly due to the adsorbed $HClO_4$ on the surface from the electrolyte.
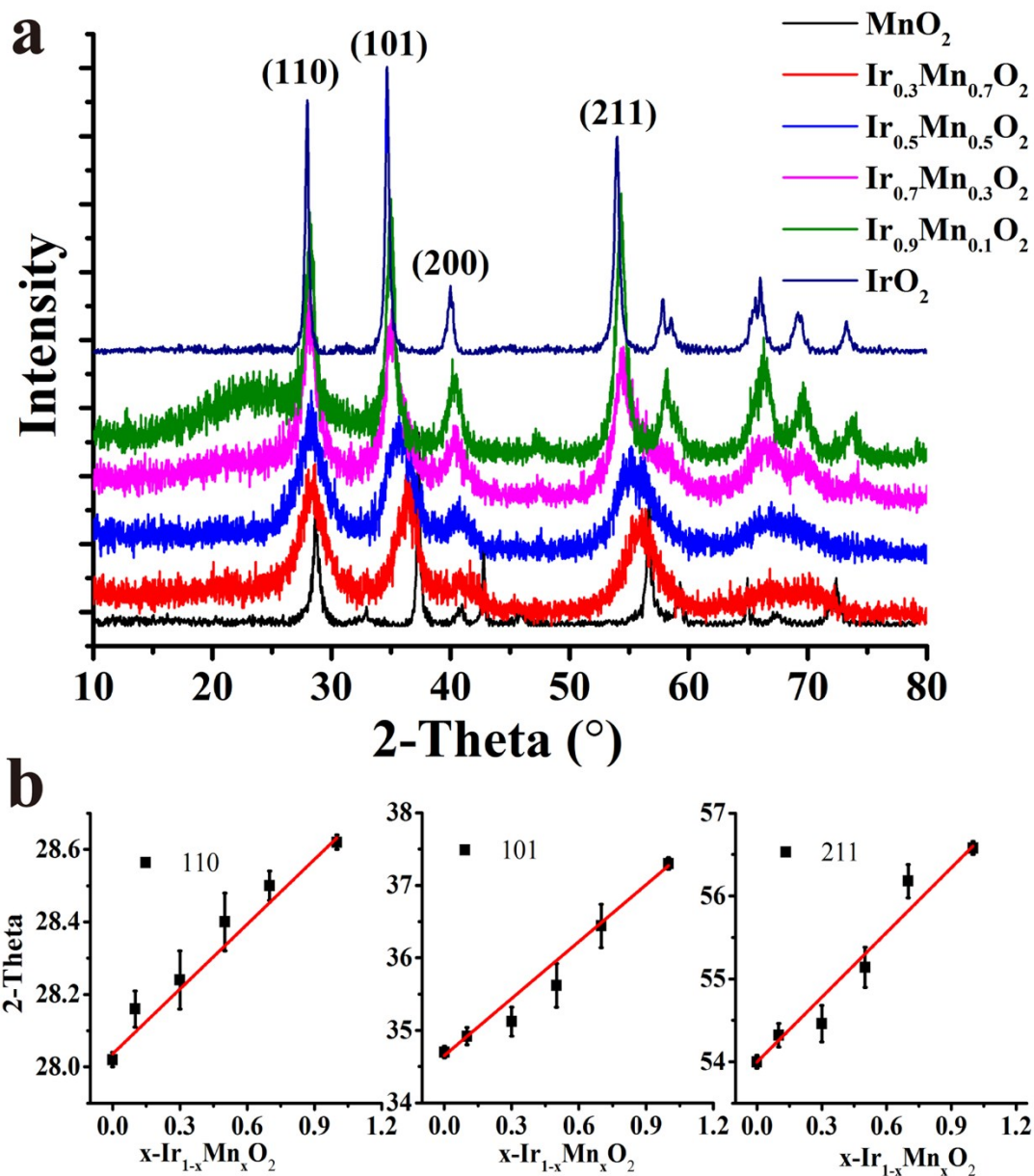
Fig.S3. (a) XRD pattern of $Ir_{1-x}Mn_xO_2$ materials. (b) The 2-theta variation with different Mn doped amount corresponding to (110), (101) and (211) planes, respectively. These variation are meet with the Vegard rule indicates that $Ir_{1-x}Mn_xO_2$ materials can form the solid solution in here.
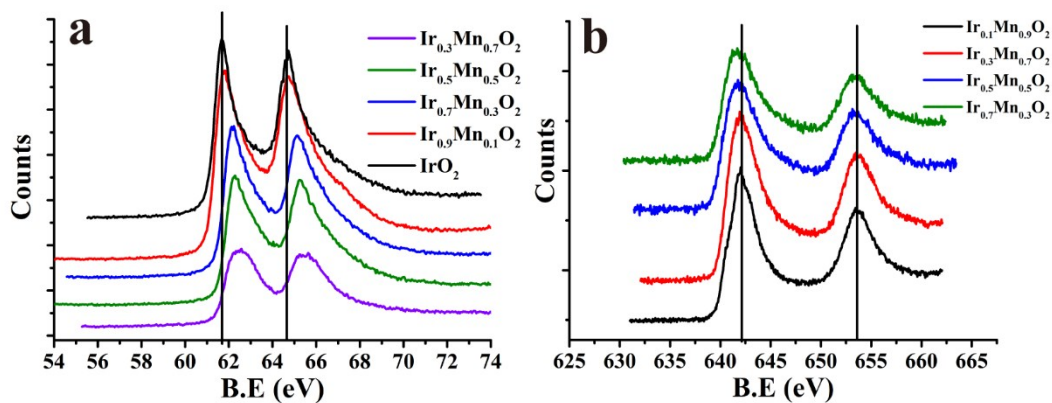
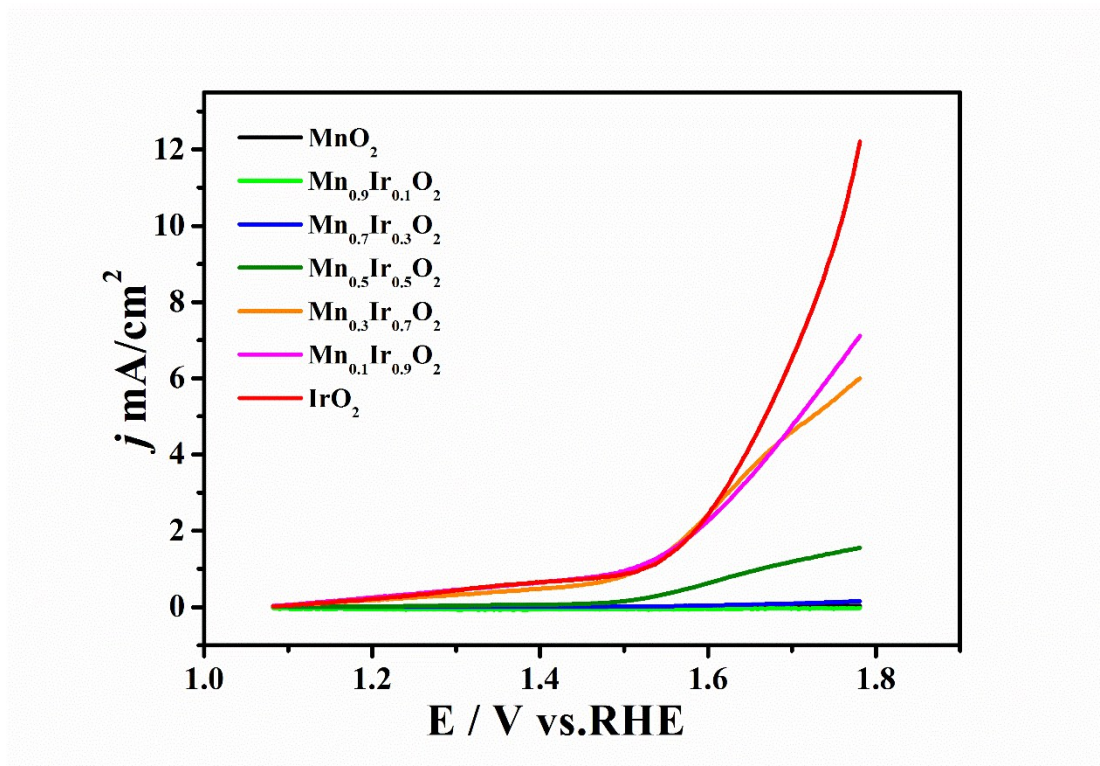**Fig.S4.** The Ir-4f (a) and Mn-2p (b) XPS for $Ir_{1-x}Mn_xO_2$ materials.

Fig.S5. OER polarization curves of $Ir_xMn_{1-x}O_2$ in 0.1M $HClO_4$. The scan rate is 25 mV/s.
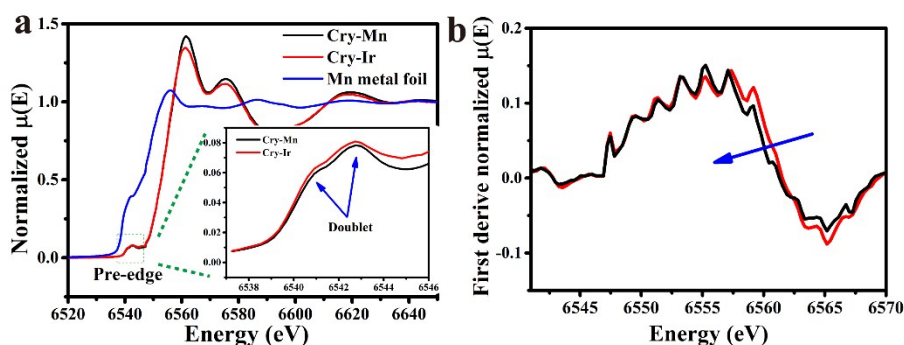
Fig.S6. (a The Mn *K*-edge XANES spectra for cry-Mn and cry-Ir, the Mn metal foil as a reference. The insert is the pre-edge spectra of cry-Mn and cry-Ir. (b) The first derivative of normalized μ(E) for cry-Mn and cry-Ir.

Table S1. The OER performance of different catalysts

Catalyst	*Activity descriptor*	Tafel slope (mV dec^{-1})
$Ru_xIr_{1-x}O_2$-presious doped	$RuO_2>Ru_xIr_{1-x}O_2>IrO_2$[2]; 1.252 V vs. Ag/AgCl gives 1 mA cm$^{-2,3}$;	37-70 @ 0.5 M H_2SO_4 ref-4
$Sn_xIr_{1-x}O_2$	30%-40% Ir mass gives maximum activity[4]; activity decreased with Sn loading[5]; IrO_2/SnO_2 (2/1) maximum activity[6]	55-60 @ 0.5 M H_2SO_4 ref-6 ; 79-305@ 0.1 M H_2SO_4 ref-8
$Cu_xIr_{1-x}O_\delta$ (0.1<x<0.3)	351-375 mV (x=0.3 maximum) gives 10 mA cm-2[1]	63-75 @0.1 M $HClO_4$
$Pt_xIr_{1-x}O_\delta$-precious doped	Activity decreased with Pt doping[7]	None @0.5 M H_2SO_4
$Co_{0.3}Ir_{0.7}O_\delta$	260 mV gives 0.5 mA cm$^{-2,8}$	40-58[8] @0.5 M H_2SO_4
$RuIrCoO_\delta$	None[9]	68 @0.5 H_2SO_4
Ni-Ir oxide	300 mV gives ~7 mA cm$^{-2,10}$	None @ 1M KOH
Cry-Ir in here		76 @0.1 M $HClO_4$
IrO_2 in here	340 mV gives 10 mA cm^{-2} None	74 @0.1 M $HClO_4$

References:

1. W. Sun, Y. Song, X.-Q. Gong, L.-m. Cao and J. Yang, *Chemical Science*, 2015, **6**, 4993-4999.
2. L.-E. Owe, M. Tsypkin, K. S. Wallwork, R. G. Haverkamp and S. Sunde, *Electrochim. Acta*, 2012, **70**, 158-164.
3. A. T. Marshall and R. G. Haverkamp, *Electrochim. Acta*, 2010, **55**, 1978-1984.
4. A. Marshall, B. Børresen, G. Hagen, M. Tsypkin and R. Tunold, *Electrochim. Acta*, 2006, **51**, 3161-3167.

5.   A. Marshall, B. Børresen, G. Hagen, M. Tsypkin and R. Tunold, *Mater. Chem. Phys.*, 2005, **94**, 226-232.

6.   J. Xu, G. Liu, J. Li and X. Wang, *Electrochim. Acta*, 2012, **59**, 105-112.

7.   K. M. Papazisi, A. Siokou, S. Balomenou and D. Tsiplakides, *Int. J. Hydrogen Energy*, 2012, **37**, 16642-16648.

8.   W. Hu, H. Zhong, W. Liang and S. Chen, *ACS applied materials & interfaces*, 2014, **6**, 12729-12736.

9.   R. G. González-Huerta, G. Ramos-Sánchez and P. B. Balbuena, *J. Power Sources*, 2014, **268**, 69-76.

10.   T. Reier, Z. Pawolek, S. Cherevko, M. Bruns, T. Jones, D. Teschner, S. Selve, A. Bergmann, H. N. Nong, R. Schlögl, K. J. J. Mayrhofer and P. Strasser, *J. Am. Chem. Soc.*, 2015, **137**, 13031-13040.

1.   L.-E. Owe, M. Tsypkin, K. S. Wallwork, R. G. Haverkamp and S. Sunde, *Electrochim. Acta*, 2012, **70**, 158-164.

2.   A. T. Marshall and R. G. Haverkamp, *Electrochim. Acta*, 2010, **55**, 1978-1984.

3.   A. Marshall, B. Børresen, G. Hagen, M. Tsypkin and R. Tunold, *Electrochim. Acta*, 2006, **51**, 3161-3167.

4.   A. Marshall, B. Børresen, G. Hagen, M. Tsypkin and R. Tunold, *Mater. Chem. Phys.*, 2005, **94**, 226-232.

5.   J. Xu, G. Liu, J. Li and X. Wang, *Electrochim. Acta*, 2012, **59**, 105-112.

6.   W. Sun, Y. Song, X.-Q. Gong, L.-m. Cao and J. Yang, *Chemical Science*, 2015, **6**, 4993-4999.

7.   K. M. Papazisi, A. Siokou, S. Balomenou and D. Tsiplakides, *Int. J. Hydrogen Energy*, 2012, **37**, 16642-16648.

8.   W. Hu, H. Zhong, W. Liang and S. Chen, *ACS applied materials & interfaces*, 2014, **6**, 12729-12736.

9.   R. G. González-Huerta, G. Ramos-Sánchez and P. B. Balbuena, *J. Power Sources*, 2014, **268**, 69-76.

10.   T. Reier, Z. Pawolek, S. Cherevko, M. Bruns, T. Jones, D. Teschner, S. Selve, A. Bergmann, H. N. Nong, R. Schlögl, K. J. J. Mayrhofer and P. Strasser, *J. Am. Chem. Soc.*, 2015, **137**, 13031-13040.